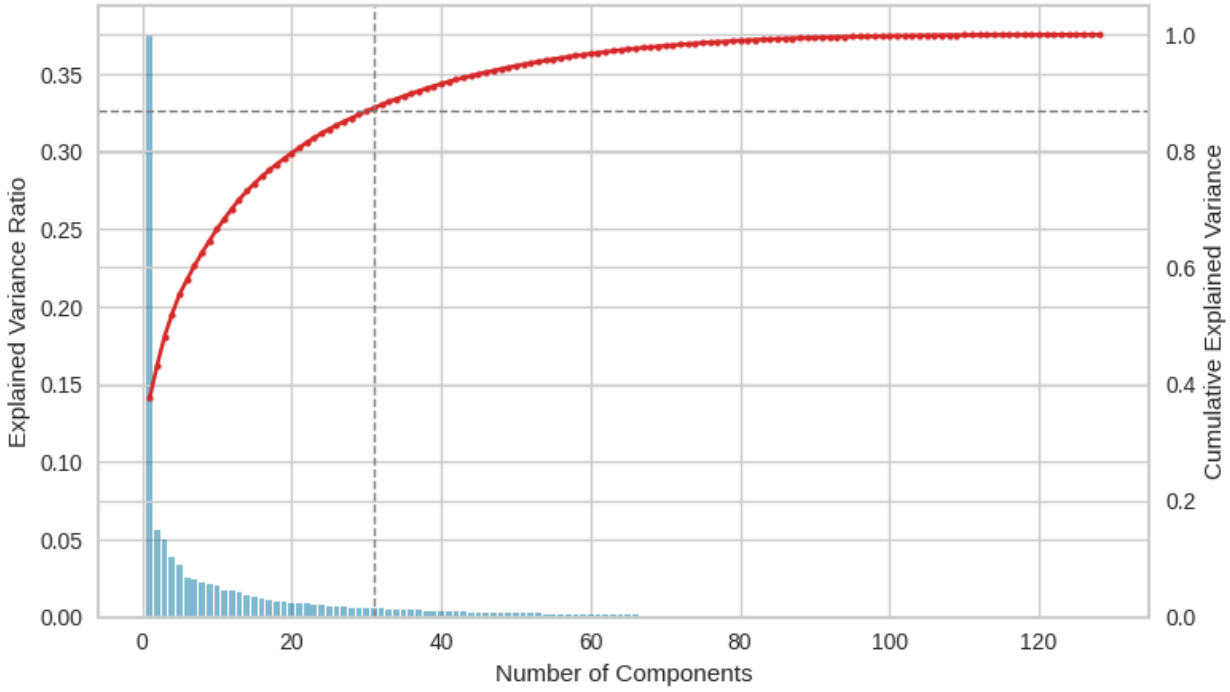
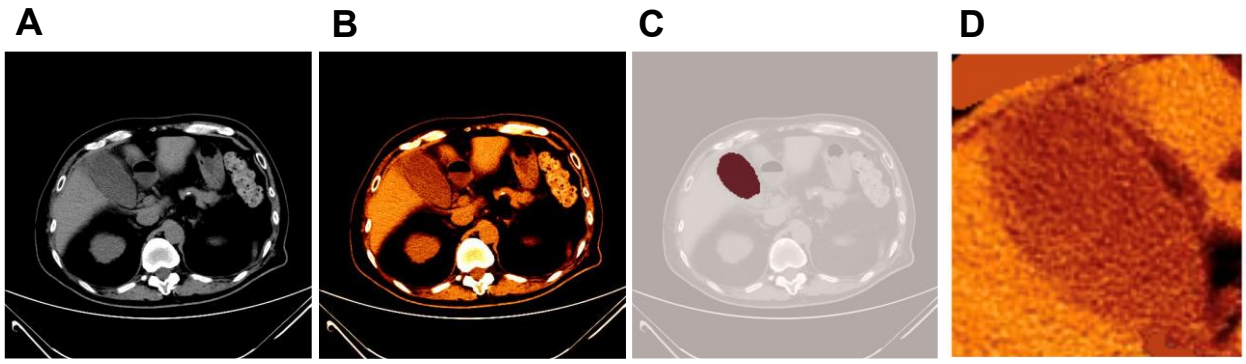
Figure S1. Cumulative explained variance of principal component analysis for image-derived features.



The bars represent the proportion of variance explained by each individual principal component, whereas the red line represents the cumulative proportion of variance explained by the components. The cumulative explained variance increased with the number of principal components, and 31 components were required to retain more than 85% of the variance.

Figure S2. Preprocessing pipeline for CT image preparation.



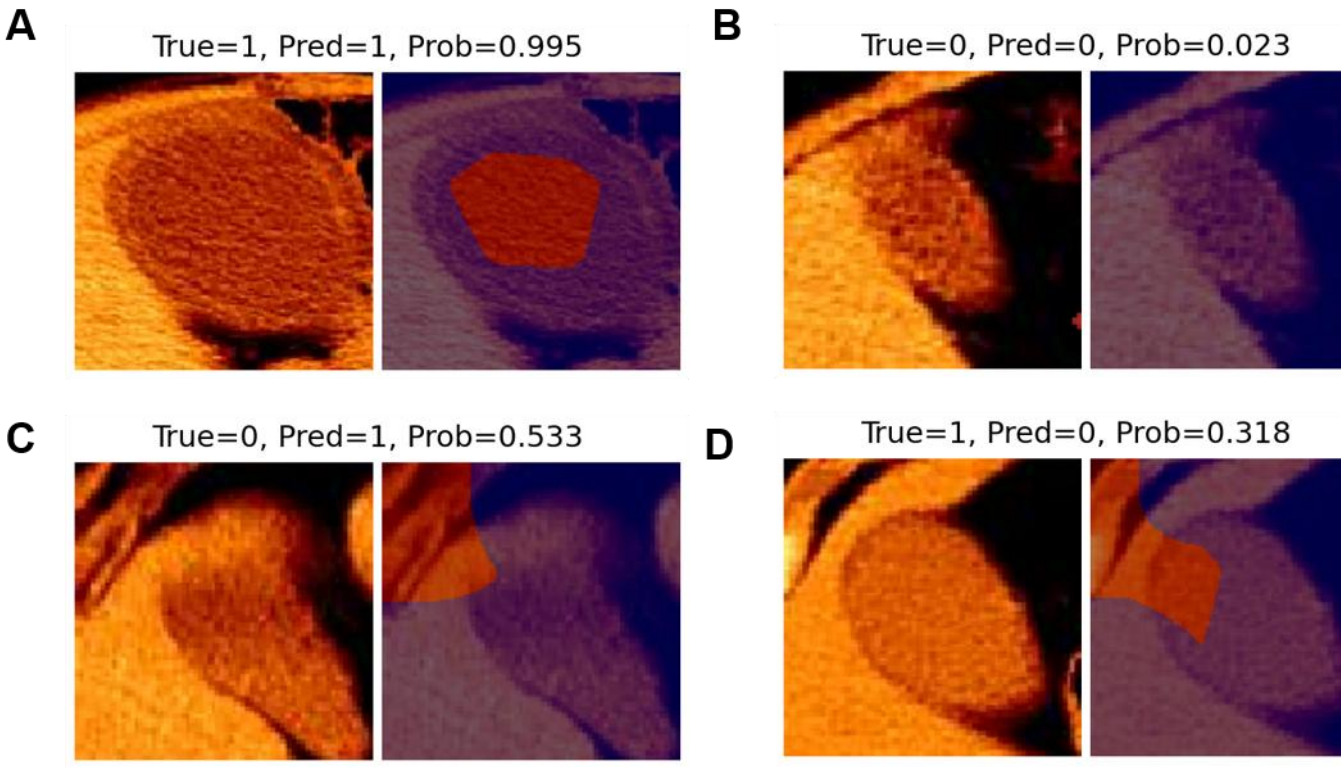
(A) Original CT image converted from DICOM to grayscale format.

(B) Corresponding image converted to an RGB (three-channel) representation.

(C) Automated gallbladder segmentation using *TotalSegmentator*, with the segmented region overlaid on the CT image.

(D) Cropped image centered on the segmented region with an additional margin, followed by correction of white saturation (blowout) artifacts.

Figure S3. Representative Grad-CAM visualizations of the image model.



(A–D) Representative cases showing input images (left) and corresponding Grad-CAM attention maps (right). Grad-CAM highlights regions contributing to the model's decision. Each panel includes the ground-truth label (True), model prediction (Pred), and predicted probability (Prob).

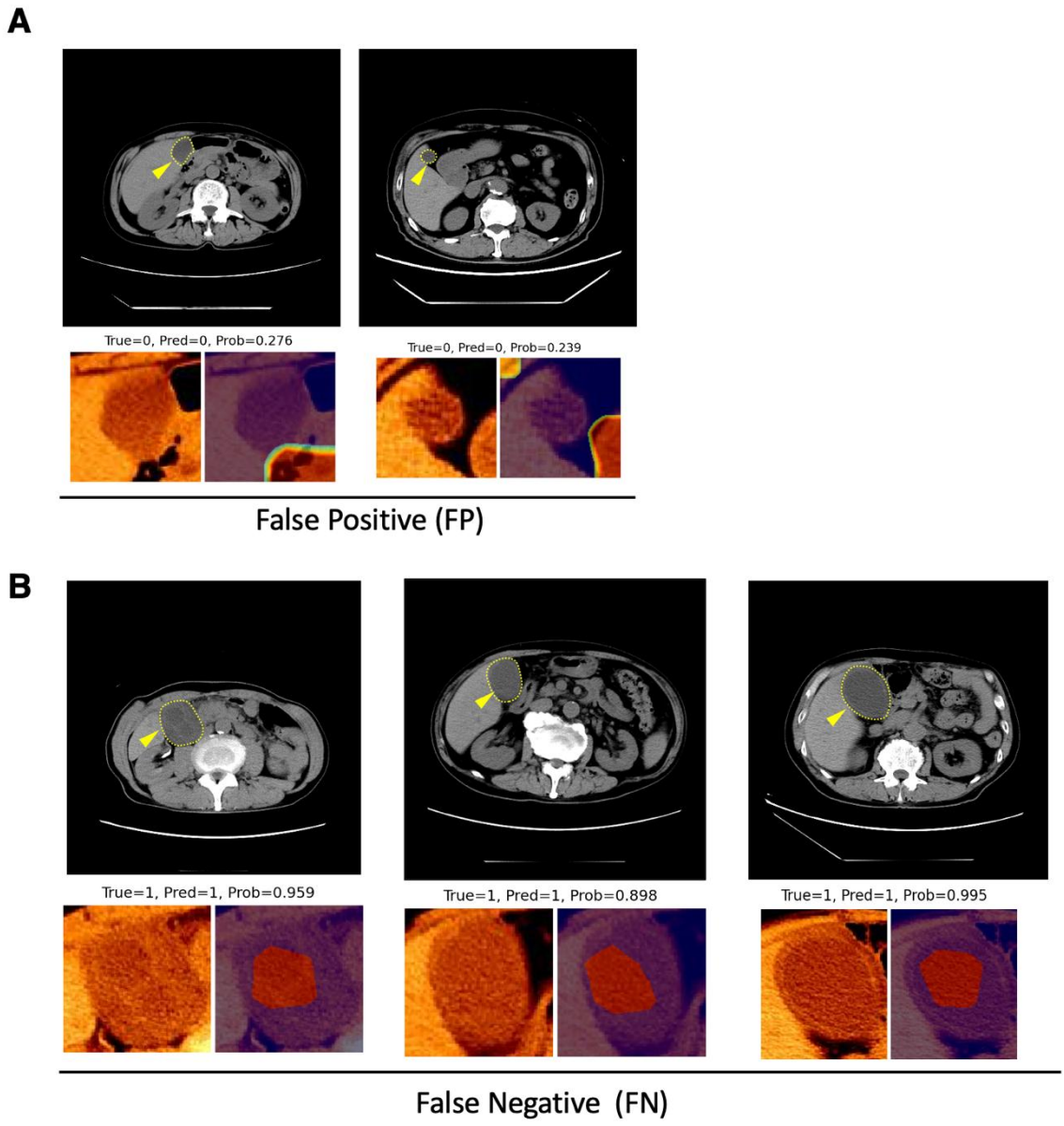
(A)True positive case.

(B)True negative case.

(C) False positive case.

(D) False negative case.

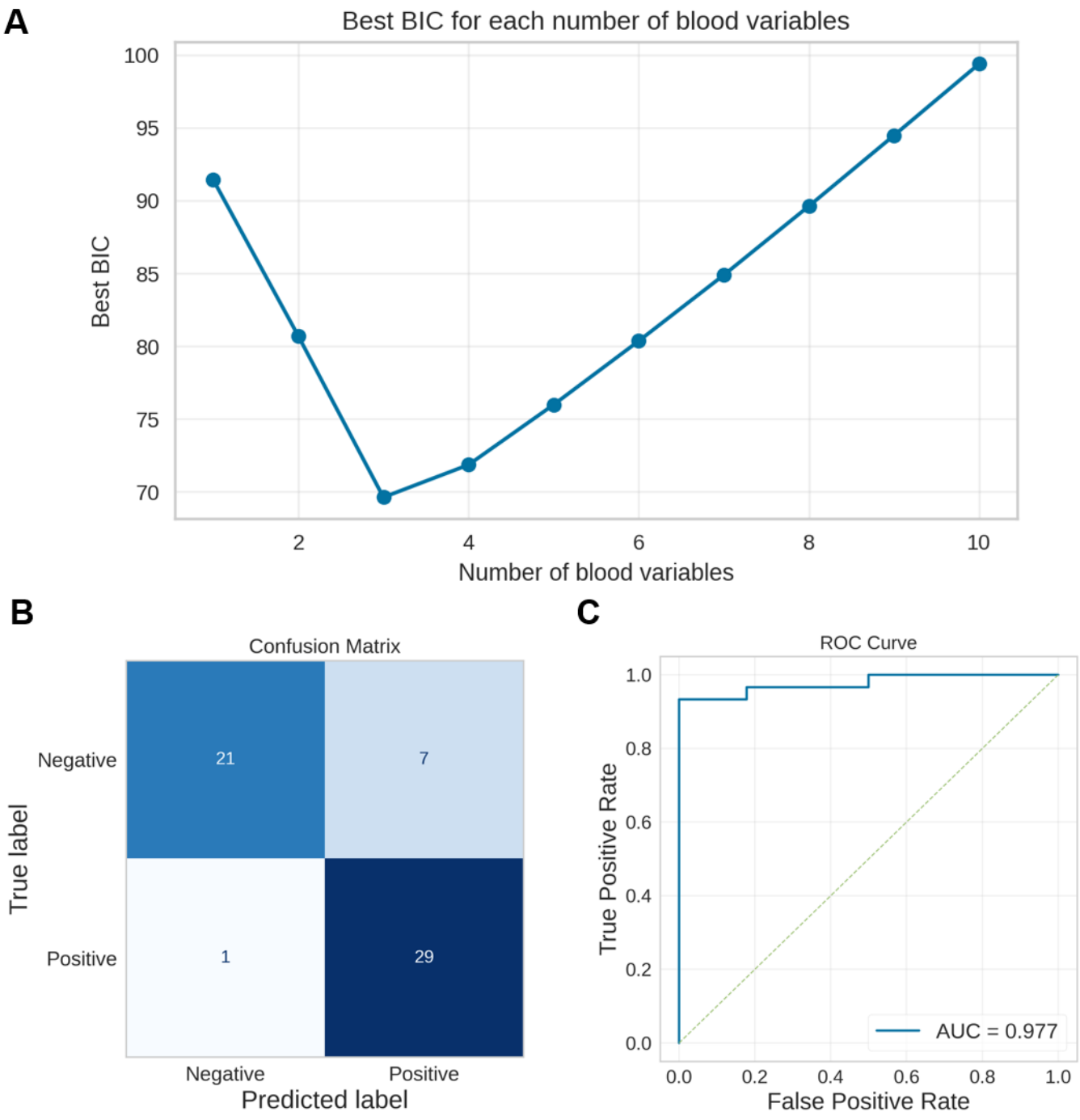
Figure S4. Representative cases illustrating discordance between blood-based predictions and image-based features.



(A) False positive cases from the blood-based model (True = 0, Pred = 1). Although classified as positive based on blood data, the corresponding CT images and Grad-CAM maps from the image-based model suggest limited or nonspecific imaging findings.

(B) False negative cases from the blood-based model (True = 1, Pred = 0). Despite misclassification by the blood-based model, the image-based model highlights regions corresponding to the gallbladder, indicating imaging features consistent with disease.

Figure S5. Model optimization and performance of the hybrid model



(A) Model selection for blood variables in the hybrid model based on the Bayesian Information Criterion (BIC). All possible combinations of blood variables (from 1 to 10 variables) were evaluated while keeping the image-derived features fixed. For each number of blood variables, the model with the lowest

BIC was selected. The optimal model was achieved with three blood variables (WBC, CRP, ALP), which yielded the minimum BIC, indicating the best trade-off between model fit and complexity. (B) Confusion matrix of the hybrid model using the optimal combination of three blood variables. (C) Receiver operating characteristic (ROC) curve of the hybrid model with the optimal three blood variables.

Although the three-variable model achieved the lowest BIC, the model incorporating all blood variables demonstrated superior predictive performance and was therefore selected as the final model for the main analysis.